Poststimulus undershoots in cerebral blood flow and BOLD fMRI responses are modulated by poststimulus neuronal activity

Karen J. Mullinger[a,1,2], Stephen D. Mayhew[b,1], Andrew P. Bagshaw[b], Richard Bowtell[a], and Susan T. Francis[a]

[a]Sir Peter Mansfield Magnetic Resonance Centre, School of Physics and Astronomy, University of Nottingham, Nottingham NG7 2RD, United Kingdom; and [b]Birmingham University Imaging Centre, School of Psychology, University of Birmingham, Birmingham B15 2TT, United Kingdom

Edited by Marcus E. Raichle, Washington University in St. Louis, St. Louis, MO, and approved July 3, 2013 (received for review December 12, 2012)

fMRI is the foremost technique for noninvasive measurement of human brain function. However, its utility is limited by an incomplete understanding of the relationship between neuronal activity and the hemodynamic response. Though the primary peak of the hemodynamic response is modulated by neuronal activity, the origin of the typically negative poststimulus signal is poorly understood and its amplitude assumed to covary with the primary response. We use simultaneous recordings of EEG with blood oxygenation level-dependent (BOLD) and cerebral blood flow (CBF) fMRI during unilateral median nerve stimulation to show that the poststimulus fMRI signal is neuronally modulated. We observe high spatial agreement between concurrent BOLD and CBF responses to median nerve stimulation, with primary signal increases in contralateral sensorimotor cortex and primary signal decreases in ipsilateral sensorimotor cortex. During the poststimulus period, the amplitude and directionality (positive/negative) of the BOLD signal in both contralateral and ipsilateral sensorimotor cortex depends on the poststimulus synchrony of 8–13 Hz EEG neuronal activity, which is often considered to reflect cortical inhibition, along with concordant changes in CBF and metabolism. Therefore we present conclusive evidence that the fMRI time course represents a hemodynamic signature of at least two distinct temporal phases of neuronal activity, substantially improving understanding of the origin of the BOLD response and increasing the potential measurements of brain function provided by fMRI. We suggest that the poststimulus EEG and fMRI responses may be required for the resetting of the entire sensory network to enable a return to resting-state activity levels.

simultaneous EEG–fMRI | event-related synchronization | rebound | alpha power | neurovascular-coupling

Blood oxygenation level-dependent (BOLD) fMRI is the foremost noninvasive technique for measuring the spatial location and intensity of human brain function (1). BOLD contrast allows information about enhanced neuronal activity to be inferred from fMRI signal increases and has been instrumental in shaping current neuroscientific understanding of how macroscopic neuronal processes give rise to complex human behavior (2). However, current interpretations of fMRI data are often limited by the assumption that there is a canonical hemodynamic response (HR) to external stimuli, which implies a fixed relationship between the two main BOLD signal components: the primary signal increase and the poststimulus undershoot. This assumption implicitly imposes a model whereby the brain's response is consistent and standardized, neglecting widespread demonstrations of the behavioral and neurobiological significance of variability in evoked brain responses (3), as well as ignoring the considerable variability in HR amplitude, morphology, and latency both between and within individuals (4, 5). While use of the canonical HR has enabled functional localization studies, its oversimplification of brain responses restricts the ability to extract the most behaviorally relevant signal modulations from the BOLD fMRI data; by definition, this requires accurate characterization of single-trial brain responses and a comprehensive understanding of the entire BOLD response time-course and its variability.

One of the most fundamental requirements is to improve the understanding of the neurophysiological origin of the poststimulus undershoot, which comprises at least half of the HR time course but is inconsistently observed in the average HR, possibly because of single-trial variability in the undershoot's shape and amplitude. The primary BOLD response indirectly reflects increases in neuronal activity via concordant increases in cerebral blood flow (CBF), blood volume (CBV), and metabolic rate of oxygen consumption ($CMRO_2$) (6, 7). The poststimulus undershoot occurs after the primary BOLD signal increase, following stimulus cessation; it is classically characterized as an average decrease in BOLD signal below prestimulus baseline, followed by a subsequent recovery to baseline. The physiological origins of the poststimulus undershoot remain unclear despite numerous studies in animals (8, 9) and humans (10–14). A number of putative mechanisms have been proposed: (*i*) poststimulus elevation of CBV, after CBF and $CMRO_2$ have returned to baseline (the balloon model) (15), implying a purely vascular origin; (*ii*) CBF returning to baseline with $CMRO_2$ remaining elevated after stimulus cessation (11, 16), possibly due to a rebalancing of ionic gradients poststimulation (16, 17); and (*iii*) a decrease in CBF below baseline accompanied by a lesser reduction in $CMRO_2$ (10, 13, 18). This mechanism is the inverse of the mechanism underlying the primary BOLD response and therefore may be driven by a decrease in neuronal activity below baseline levels.

Recent work presents strong evidence of an alteration in $CMRO_2$ relative to baseline during the poststimulus period (11, 16), thus excluding mechanism *i* as the sole cause of the BOLD poststimulus undershoot. However, it is currently not possible to discriminate between mechanisms *ii* or *iii* due to contradictory reports of either a reduction (10, 13) or no change (11) in CBF during the BOLD poststimulus undershoot period. This ambiguity may be due to spatial variability in the poststimulus CBF and CBV responses, as recently shown in animal studies (8, 9), the low sensitivity of the arterial spin-labeling (ASL) sequences used to measure CBF, or suboptimal sequential acquisition of BOLD and CBF data. Simultaneous acquisition of BOLD, CBF, and EEG integrates information from both neuroelectric and hemodynamic signals, thus providing an important conceptual

Author contributions: K.J.M., S.D.M., A.P.B., R.B., and S.T.F. designed research; K.J.M. and S.D.M. performed research; K.J.M. and S.D.M. analyzed data; and K.J.M., S.D.M., A.P.B., R.B., and S.T.F. wrote the paper.

The authors declare no conflict of interest.

This article is a PNAS Direct Submission.

Freely available online through the PNAS open access option.

[1]K.J.M. and S.D.M. contributed equally to this work.

[2]To whom correspondence should be addressed. E-mail: karen.mullinger@nottingham.ac.uk.

This article contains supporting information online at www.pnas.org/lookup/suppl/doi:10.1073/pnas.1221287110/-/DCSupplemental.

framework for elucidating the origins of the BOLD undershoot, and in particular to determine whether poststimulus neuronal modulations contribute to the undershoot (mechanism *iii*).

The hypothesis that a reduction in neuronal activity, often conceptualized as neuronal inhibition, underlies the poststimulus undershoot is supported by primate electrophysiological recordings. In brain regions exhibiting a positive primary BOLD response to a visual stimulus (19), neuronal activity was shown to decrease below prestimulus baseline levels for up to 10 s (19) after cessation of the visual stimulus. Therefore, accounting for the hemodynamic delay, this reduction in neuronal activity is a highly plausible source of the BOLD poststimulus undershoot. Furthermore, in regions where the primary BOLD response to the stimulus decreased compared with baseline levels (negative BOLD response) (20, 21), the neuronal activity following stimulus cessation increased above baseline, causing a BOLD poststimulus overshoot (19). A poststimulus overshoot following a negative primary BOLD response has also been reported in human visual (21) and somatosensory (20) cortices. Shmuel et al. (19) proposed that a decrease (increase) in neuronal activity triggering a decrease (increase) in CBF may underlie the BOLD poststimulus undershoot (overshoot), providing further support for mechanism *iii*.

Poststimulus changes in oscillatory neuronal activity relative to prestimulus baseline levels have also been measured noninvasively in humans using EEG and magnetoencephalography (MEG) (22, 23). The widely reported poststimulus event-related synchronization (PERS), or rebound, consists of an increase in power lasting a few seconds in the alpha (8–13 Hz) and/or beta (13–30 Hz) frequency bands following motor task performance, sensorimotor, or visual stimulation (22–24). Alpha and beta rhythm event-related synchronization (ERS) are believed to underlie functional inhibition (24–26). The mu rhythm is a typical example of the alpha rhythm found in the sensorimotor cortex. The amplitude of both the PERS (24, 27) and poststimulus BOLD response (10, 13) is modulated by stimulus intensity and duration; we hypothesize that this reflects an underlying correlation between hemodynamic and electrophysiological responses, and that the neuronal activity that underlies the EEG/MEG rebound is also the source of the BOLD poststimulus undershoot and perhaps suggests an inhibitory role of this fMRI response. A close correspondence between the spatial location of the beta-PERS and primary positive BOLD response to visual and motor stimuli (24) suggests that these reflect activity from a common neuronal population. However, the correlation between the amplitude of PERS (or any other neuronal activity) and the BOLD poststimulus undershoot has not been investigated.

This study investigates the neuronal contribution to the poststimulus HR by analyzing simultaneously recorded EEG-BOLD-CBF sensorimotor cortex responses to median nerve stimulation (MNS). The unique and powerful combination of three noninvasive neuroimaging measures enables the most detailed investigation to date of the neurovascular coupling underlying the poststimulus response in humans. We use a trial-by-trial analysis to demonstrate the contribution of neuronal (EEG), metabolic ($CMRO_2$), and hemodynamic (CBF) response variability to the poststimulus BOLD signal. We observe significant positive and negative primary BOLD and CBF responses in contralateral and ipsilateral sensorimotor cortex, respectively. In both regions, BOLD and CBF poststimulus signal directionality varied from trial-to-trial between an undershoot or overshoot, with an amplitude that correlated negatively with PERS mu power. This work provides conclusive evidence that increases/decreases in the poststimulus BOLD signal reflect commensurate changes in neuronal activity, metabolism, and CBF.

Results

Correlations between poststimulus EEG mu power and BOLD and CBF responses were assessed. For each subject, trials were sorted into quartiles [lower (0–25%), median (37.5–62.5%), and upper (75–100%)] according to the average PERS mu power during a 10.5- to 20-s time window (relative to the 0- to 10-s period of MNS). Single-trial BOLD and CBF time courses were then correspondingly sorted and averaged within quartiles and across subjects to determine the poststimulus HR modulation. Additionally, the HRs were sorted according to average mu power calculated during stimulus response (0–9.5 s) and control (25–29.5 s) windows and compared with the PERS mu-power sorting effects. Stimulus-related changes in beta power were also investigated, but not consistently found across subjects. We therefore focused on the robust mu power changes in the remaining analysis.

Sorting EEG Mu Power. Fig. 1 shows the group average time-course of mu power for each quartile when sorted according to stimulus response, PERS, and control window. Distinct differences in the mu power between quartiles specific to the time window of sorting, and independent of the remainder of the time course, are seen. No significant correlation between PERS mu power and either stimulus response or control window mu power was observed in any subject (minimum P value = 0.18). Fig. S1 shows the significant difference in stimulus response, PERS, and control window mu power between quartiles, and the variability across subjects.

Close Spatial Correspondence Between EEG-Mu, and BOLD and CBF Responses to MNS. The primary BOLD/CBF signal response (peak latency ~10 s) to MNS was positive in contralateral primary sensorimotor cortex (Fig. 2, red) and negative in the ipsilateral primary sensorimotor cortex (Fig. 2, blue). A close spatial correspondence was observed between the group conjunction of the regions of significant contralateral/ipsilateral BOLD and CBF response to MNS and the beamformer group average T-stat map of changes in oscillatory mu power during the stimulus response window.

Modulation of HRs by PERS Mu Power. Fig. 3 shows that during the poststimulus period (20–30 s), both the contralateral and ipsilateral BOLD amplitude, and contralateral CBF amplitude were negatively correlated with PERS mu power. Upper quartile mu power (shown in red) corresponded to an fMRI poststimulus undershoot, whereas the lower quartile mu power (shown in black) corresponded to an fMRI poststimulus overshoot. Two-way repeated-measures ANOVA showed a significant interaction between time and sorting according to PERS quartile mu power for contralateral [$F(1.8, 18.2) = 3.47$, $P = 0.016$] and ipsilateral BOLD [$F(1.5, 15.6) = 3.88$, $P = 0.009$] and contralateral CBF [$F(2.3, 23.0) = 3.29$, $P = 0.026$] time course amplitudes, indicating that the modulation of the HR amplitude by PERS mu quartile was dependent on the time point within the response. Testing for differences between quartiles at individual time points revealed a significant ($P < 0.05$) effect of PERS mu power on poststimulus

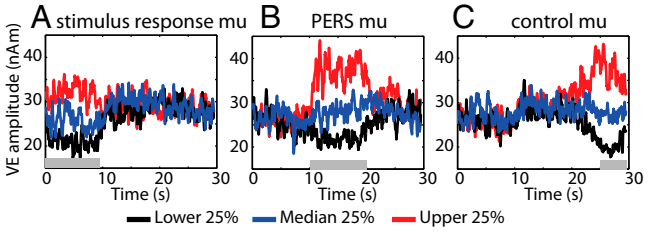

Fig. 1. Group average of the Hilbert envelope of virtual electrode mu time course for each quartile according to sorting single trials by the average mu power during stimulus response (0–9.5 s; *A*), PERS (10.5–20 s; *B*), and control (24.5–29.5 s; *C*) time windows. Colored lines denote lower (black), median (blue), and upper (red) quartiles. Gray shaded bars denote the duration of the sorting window.

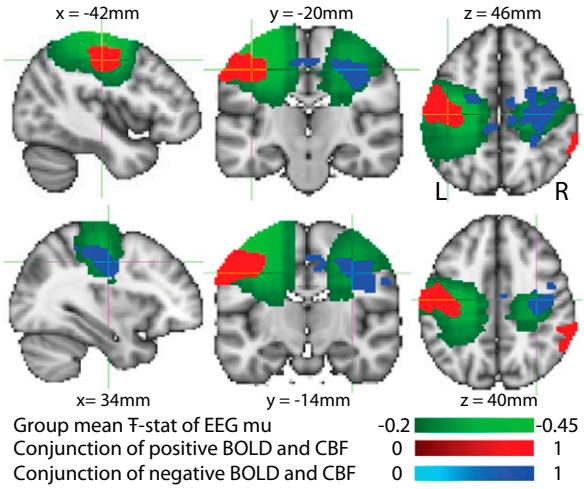

Fig. 2. Conjunction of the group fixed-effects, contralateral positive (red) and ipsilateral negative (blue) primary BOLD ($P < 0.05$, familywise error corrected) and CBF ($P < 0.001$, uncorrected) responses superimposed upon the group average Ŧ-stat of the EEG mu response (green) to MNS (active (0–9.5 s), passive (20–29.5 s) windows). Cross-hairs are centered on the peak BOLD voxel in the contralateral and ipsilateral conjunction masks, respectively.

contralateral BOLD (23.5–29.5 s) and CBF (25–28.5 s) amplitudes (Fig. 3 *A* and *C*). In addition, BOLD (upper quartile) and CBF (upper and lower quartiles) contralateral poststimulus responses measured from individual subjects were found to be significantly ($P < 0.05$, Student *t* test) different from zero across the group. A significant difference in poststimulus amplitude between quartiles was also observed for the ipsilateral BOLD time course (24.5–29.5 s; Fig. 3*B*), but not for the ipsilateral CBF data (Fig. 3*D*). We also found an increase in the primary peak amplitude and a significantly greater lag of the falling edge of each of the contralateral BOLD (~10.75–18.75 s), contralateral CBF (~12.5–16.5 s), and the ipsilateral BOLD (8–14.25 s) responses in trials with higher PERS mu power. The local minima/maxima in the lower quartile contralateral/upper quartile ipsilateral BOLD responses at 19.2 s were not found to be significantly

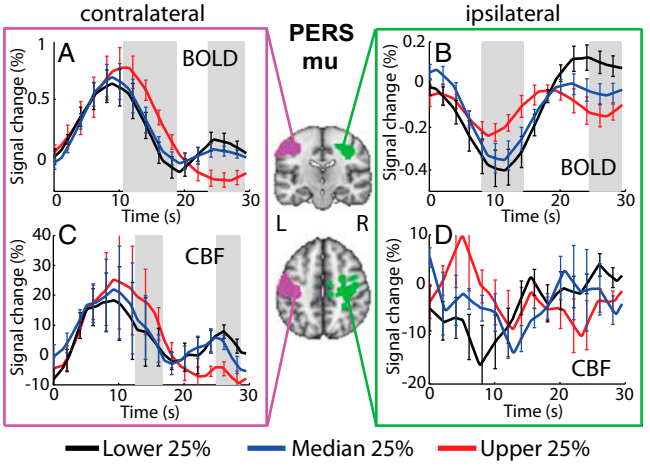

Fig. 3. BOLD and CBF HRs sorted according to quartiles of PERS (10.5–20 s) mu power for contralateral (*A* and *C*) and ipsilateral (*B* and *D*) regions. Center images show conjunction of contralateral (pink) and ipsilateral (green) group BOLD and CBF T-stat maps. Gray bars show significant ($P < 0.05$, repeated-measures ANOVA) differences in HR amplitude between lower (black), median (blue), and upper (red) quartiles. Error bars indicate SEM.

($P < 0.05$, Student *t* test) different from zero, and therefore we interpret this as a turning point, rather than early undershoot/overshoot.

Modulation of HRs by Stimulus or Control Mu Power. Two-way repeated-measures ANOVA showed a significant interaction between time and sorting according to stimulus response mu power for contralateral [$F(1.89, 18.9) = 2.762$, $P = 0.036$] and ipsilateral [$F(2.14, 21.4) = 3.38$, $P = 0.02$] BOLD time course amplitudes. Only the amplitude of the rising edge (3–7.5 s) of the primary contralateral BOLD response was significantly different between stimulus response mu power quartiles (Fig. 4*A*). In addition, the primary peak amplitude of the ipsilateral BOLD response (~11.25–13.5 s; Fig. 4*B*) was significantly larger for the upper mu quartile. No significant effects were found in the CBF responses (Fig. 4 *C* and *D*). We found no significant differences in the poststimulus BOLD or CBF signal amplitude across quartiles when fMRI trials were sorted according to stimulus response (Fig. 4) or control window (Fig. S2) mu power, providing further evidence that our findings truly reflect a correlation between the poststimulus neuronal and fMRI signals.

$CMRO_2$ Changes During the Poststimulus Period. $CMRO_2$ was calculated during the poststimulus period from the amplitude of BOLD and CBF undershoots and overshoots for each subject, using the Davis model (28) so as to identify the change in metabolic demand associated with lower and upper quartiles of PERS mu power. Table 1 shows that the observed BOLD poststimulus undershoot (Fig. 3*A*, red line) is caused by a decrease in CBF and $CMRO_2$, whereas the poststimulus overshoot (Fig. 3*A*, black line) is caused by increases in CBF and $CMRO_2$. The $CMRO_2$ change during the poststimulus period is less than half of that measured during the primary response period (Table 1), as expected due to the larger primary BOLD and CBF responses. The difference in calculated $CMRO_2$ for the upper and lower quartiles of PERS mu power was significant ($P < 0.05$) for M of 10.6 and higher, and showed a trend ($P < 0.1$) for the lowest M value.

Discussion

Neuronal Origin of the BOLD Poststimulus Undershoot. This study provides evidence that the amplitude of the poststimulus BOLD signal is a hemodynamic signature of poststimulus changes in neuronal mu-band oscillatory activity. The commonly reported poststimulus undershoot is not consistently an undershoot. Rather, single-trial analyses reveal the directionality of this signal is dependent on the synchrony of 8- to 13-Hz poststimulus neuronal activity. Following 10 s of sensorimotor stimulation, both contralateral (positive) and ipsilateral (negative) fMRI response regions exhibited BOLD and CBF poststimulus undershoots (20–30 s) in trials with high PERS mu power (10–20 s), accompanied by reduced levels of $CMRO_2$ (20–30 s) compared with baseline. Trials with low PERS mu power exhibited BOLD and CBF poststimulus overshoots accompanied by increased levels of $CMRO_2$ (Table 1).

Simultaneous BOLD-CBF recordings allow us to conclude that poststimulus BOLD signals originate from proposed mechanism *iii* (decrease in neuronal activity and accompanying reduction in CBF) rather than mechanism *ii* (ionic rebalancing and no change in CBF). $CMRO_2$ changes cannot be measured directly; therefore, inferences based on calculations, such as the Davis model (28), are necessary. In the circumstance of large reductions in BOLD with small reductions in CBF, the Davis model predicts an increase in $CMRO_2$ (29) and suggests mechanism *ii* would pertain. However, it is difficult to develop a credible biomechanical mechanism that would produce a reduction in CBF without a reduction in $CMRO_2$. The magnitude of the CBF change observed in our data strongly suggests that a decrease in $CMRO_2$ occurs concurrently with a poststimulus

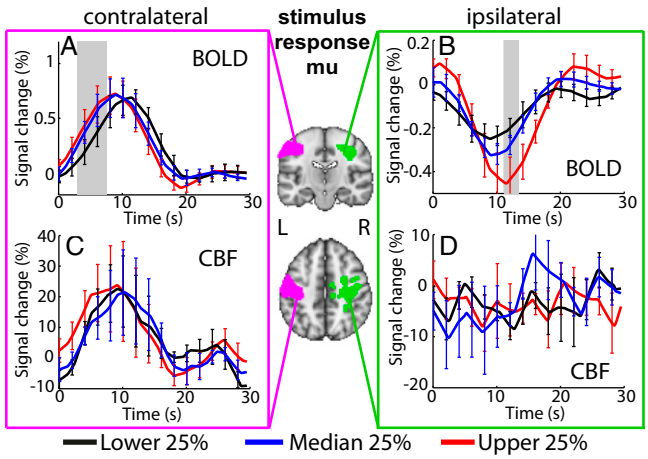

Fig. 4. BOLD and CBF HRs sorted according to quartiles of stimulus response (0–9.5 s) mu power for contralateral (*A* and *C*) and ipsilateral (*B* and *D*) regions. Center images show conjunction of contralateral (pink) and ipsilateral (green) group BOLD and CBF T-stat maps. Gray bars show significant ($P < 0.05$, repeated-measures ANOVA) differences in HR amplitude between lower (black), median (blue), and upper (red) quartiles. Error bars indicate SEM.

BOLD undershoot, supporting the hypothesis that the poststimulus fMRI signal is neuronal in origin. These results extend invasive work in primates (19) and indicate that the previously proposed mechanism *iii* underlies the BOLD poststimulus response. Our findings indicate that the poststimulus response originates from a similar mechanism to that of the primary BOLD response, and is neuronal in origin.

Are the Davis and Baseline Assumptions Correct for Poststimulus Responses? Implications for $CMRO_2$ Estimation. The mechanism originally proposed for the BOLD poststimulus undershoot was based on slow vascular compliance, with CBV remaining elevated after CBF and $CMRO_2$ returned to baseline (15, 30). Though our results refute this possibility due to the concurrent poststimulus reduction in CBF and BOLD, and hence $CMRO_2$, we have not measured CBV and cannot rule out slow poststimulus changes in CBV due to vascular compliance effects. However, a slow recovery in CBV can be associated only with the poststimulus undershoot. Our data show that the occurrence of a poststimulus increase in BOLD signal (an overshoot) is equally as likely as an undershoot (Fig. 3). A purely hemodynamic explanation of such an overshoot would require either a poststimulus reduction in CBV below the prestimulus baseline level, for which no evidence exists, or a slower return to baseline of CBF than CBV. These circumstances are highly unlikely, and therefore we suggest that the changes in neuronal activity drive the $CMRO_2$ and CBF change and consequently the BOLD time course (Fig. 3).

Alternative definitions of the baseline for CBF and BOLD signals may also influence the $CMRO_2$ changes calculated. The optimal definition of a baseline signal in BOLD data is not straightforward because the brain is never truly at rest (31, 32). Here we calculate the mean baseline value for each subject from the average signal in the 24- to 30-s time period, and use this value to convert all single trials to percent signal change. Using a different temporal interval to define the baseline would affect the measurement of fMRI response amplitude and calculated $CMRO_2$ change in a manner that is systematic across trials. Therefore, the correlation between the BOLD and CBF responses (and calculated $CMRO_2$) in the poststimulus period with trial-by-trial variability in PERS mu power would be unaffected by changes in baseline, and thus a neuronal origin of the poststimulus fMRI response would still be implied if a different temporal window were used for the baseline calculation.

Because the temporal dynamics of CBF and CBV may be altered during the poststimulus period (e.g., CBV remains elevated poststimulation, but CBF decreases below baseline) (10), it is also possible that the value of the Grubb coefficient, α (used to couple CBV and CBF), applied in the Davis model during the primary response period ($\alpha = 0.2$) (10), is not valid poststimulus. Assuming that following the positive primary response CBV either returns to baseline immediately ($\alpha \sim 0$) or remains elevated due to slow changes in vascular compliance ($\alpha < 0$), then the magnitude of the calculated poststimulus change in $CMRO_2$ will exceed the values shown in Table 1. Table 1 also shows that the calculated $CMRO_2$ changes are dependent on M. As a result, the difference in $\Delta CMRO_2$ between PERS mu quartiles was not found to be significant at the lowest M value. However, for higher values of M, a significant difference was observed, which would be exacerbated by lower values of α. Therefore, our data indicate that regardless of the coupling between CBF and CBV, there is a decrease in $CMRO_2$ when a poststimulus undershoot occurs and an increase in $CMRO_2$ when a poststimulus overshoot is observed, further supporting the hypothesis that the poststimulus fMRI signal is neuronal in origin.

Functional Interpretation of the Poststimulus fMRI Signal. This study has wider implications in understanding the relationship between localized, transient brain responses and the dynamics of ongoing activity across functional networks. We demonstrate that trials with high PERS mu power exhibit a poststimulus undershoot (Fig. 3, red lines), and trials with low PERS mu power exhibit a poststimulus overshoot (Fig. 3 black lines) in both hemispheres. Therefore, the poststimulus fMRI response is modulated bilaterally by the EEG mu oscillation and exhibits the same directionality in both the contralateral and the ipsilateral somatosensory cortices, despite the opposite directionality of the primary response in the two hemispheres. This finding that the entire BOLD response time courses in positive and negative primary BOLD regions are not simple mirror images of one another for individual trials is contrary to, and advances, the current theory that a positive/negative primary BOLD response

Table 1. Mean percentage change in BOLD, CBF, and $CMRO_2$ responses relative to baseline in the contralateral (positive) regions of interest during the poststimulus period (20–29.5 s) sorted according to the PERS mu power quartiles, and primary response period (0–20 s) averaged across all trials

Hemodynamic parameter		Upper PERS mu power quartile (undershoot)	Lower PERS mu power quartile (overshoot)	Mean primary BOLD response
% ΔBOLD		−0.20 ± 0.06	0.13 ± 0.08**	0.7 ± 0.2
% ΔCBF		−7 ± 3	6 ± 3**	22 ± 13
% $\Delta CMRO_2$	M = 6	−3 ± 3	3 ± 2*	6 ± 7
	M = 10.6	−4 ± 2	4 ± 2**	11 ± 9
	M = 14.9	−5 ± 2	4 ± 2**	13 ± 9

Values are averages over all subjects with the associated SE given. Significance of the difference between upper and lower quartiles (paired *t* test): $^{**}P < 0.05$ and $^{*}P < 0.1$.

is associated with a poststimulus undershoot/overshoot (19, 20). The demonstration that the poststimulus fMRI signal reflects a dynamic neuronal response that is manifested bilaterally as a positive or negative fMRI signal from trial-to-trial provides an enhanced conceptual understanding of the switching between the task-active state and resting state.

This study shows that poststimulus neuronal activity has functional significance across the entire network recruited by the experimental task, and we hypothesize that this represents a physiological index of the fundamental transition from active stimulus processing to bilateral resetting of the network post-stimulation, and facilitates the return of the network to its resting state where fluctuations in neuronal activity are correlated between regions of functionally connected networks (33, 34). The time scale (~10-s duration) and low frequency of the PERS mu is indicative of functional integration across a widespread network rather than localized cortical signaling (35), probably driven by thalamocortical circuits (35). The importance of macroscale network activity in supporting brain function is becoming increasingly clear (36). However, little is known about the mechanisms controlling the fundamental transition between task processing and the resting state. Our study postulates the dynamics of poststimulus responses as a method by which to study these processes.

Fluctuations in the power of oscillatory EEG rhythms are coordinated by balanced activity between inhibitory and excitatory neuronal populations. Decreases in alpha (8–13 Hz) power reflect increases in cortical excitability with ERS of the alpha rhythm (of which the mu rhythm is an example) believed to underlie functional inhibition (26, 37). Mu and beta PERS follow the termination of movement or tactile stimulation and have been suggested to reflect the reduction of excitation (38) or inhibition of activity below resting baseline (39, 40). Similar trial-to-trial modulations of mu are reported bilaterally, although strongest in contralateral cortex (41); therefore, we propose that mu PERS activity influences $CMRO_2$, thus modulating poststimulus fMRI responses bilaterally.

We hypothesize that our findings can be generalized beyond the somatosensory system and represent a common response property of primary visual and motor sensory cortex where both fMRI undershoots and EEG/MEG PERS have been observed (13, 24, 38, 42–45). However, we do not suggest that alpha frequency activity is the sole neuronal origin of the poststimulus fMRI response. Across a number of studies, including this one, it is clear that the ratio of alpha/beta PERS varies between stimulus modalities (motor, somatosensory, and visual) and passive vs. active task responses (22, 24). The poststimulus balance of excitation/inhibition and the frequency of neuronal activity are therefore likely to depend on the stimulus modality, and in different experimental paradigms beta PERS could contribute to bilateral poststimulus fMRI signal modulations. This dependence on stimulus properties and cortical region may explain why the poststimulus undershoot is less consistently observed across studies than the primary positive response.

Sources of Variability in the Primary BOLD Response. The increase in lag and peak amplitude of the primary BOLD and CBF responses (8–20 s) with increasing PERS mu power (Fig. 3) is not likely to originate from PERS mu activity (10–20 s), because in the fMRI data this effect would appear later due to the inherent hemodynamic delay. Upper quartile PERS mu is linked with primary BOLD response amplitudes that are more positive bilaterally (Fig. 3 *A* and *B*, red curves) than those occurring during lower quartile PERS mu trials. We attribute this finding to the occurrence of more energetically demanding neuronal processes during stimulation that precedes upper quartile PERS mu. The bilateral correlation between the primary response and PERS mu is analogous to the modulation of the poststimulus fMRI responses. We hypothesize that PERS mu indexes, and may be dependent upon, a subcomponent of the neuronal response during stimulation that modulates the primary positive and negative fMRI responses but does not determine their overall directionality. The presence of additional neuronal signal components during stimulation would explain the discrepancy between the correlation of primary and poststimulus BOLD amplitudes and lack of correlation between stimulus and PERS mu. The complexity of the neuronal processes underlying stimulus responses is demonstrated by findings that activity across multiple frequency bands contributes to the generation of the primary BOLD response (46). Additionally, alpha (mu) frequency EEG activity probably reflects a superposition of multiple generators, which may be differentially modulated during stimulation (47, 48), thus potentially explaining the lack of correlation between stimulus mu and fMRI signals observed here.

We therefore suggest that PERS mu reflects the poststimulus output of a bilateral sensorimotor neuronal network whose activity is continuous throughout the entire trial duration and is superimposed on the lateralized activity in other frequency bands during stimulation (primarily gamma, which is closely related to BOLD signal) (7) that determine the directionality of the primary BOLD response. The local sensorimotor neuronal population activity increases with stimulus intensity/duration, thus increasing the magnitude of both the primary positive and negative BOLD responses (21, 49). However, the constant amplitude stimuli delivered here results in an increase in the amplitude of the positive primary BOLD response and a decrease in the amplitude of the negative primary BOLD response in trials with high PERS mu power (Fig. 3), which we propose is due to ongoing activity in the bilateral sensorimotor network. We suggest that during the poststimulus period, bilateral synchrony of mu is restored, regardless of stimulation intensity/duration, as the stimulus driven neuronal populations become quiescent; this results in a coherent EEG mu oscillation across the entire network and the bilateral poststimulus fMRI response modulations we observe.

Conclusion

We have used multimodal neuroimaging to show that the primary and poststimulus BOLD responses are generated by similar underlying mechanisms and represent hemodynamic signatures of distinct neuronal processes. The BOLD poststimulus response can exhibit either an undershoot or an overshoot, which is associated with a concurrent decrease/increase in CBF, a decrease/increase in $CMRO_2$, high/low PERS mu, and cortical inhibition/excitation, respectively. The same effect is observed in positive or negative primary BOLD response regions. This finding challenges the current consensus that the poststimulus response is simply a coupled subcomponent of the primary BOLD response. We suggest that modeling fMRI data with the conventional canonical HR disregards important functional information contained in trial-by-trial variability. Relating poststimulus changes in BOLD signal to neuronal activity allows exploitation of the undershoot/overshoot component of the BOLD response for localizing brain activity; this increases the available temporal information concerning stimulus responses, and extends the neurobiological responses that can be studied, such as the resetting of the entire sensory network to enable a return to resting-state activity levels.

Materials and Methods

Acquisition. fMRI and EEG data were acquired simultaneously using a Philips Achieva 3T MR scanner and a 64-channel EEG system (Brain Products). A flow-sensitive alternating inversion recovery (FAIR) FAIR double-acquisition background suppression (50) sequence was used for simultaneous acquisition of background-suppressed ASL and BOLD data. This study was conducted with the approval of the University of Nottingham Medical School ethics committee, and all subjects gave informed consent. MNS was applied to the right wrist of 18 right-handed subjects at each individual's motor threshold. Data were recorded over 40 blocks (10 s/20 s MNS/rest). The duration of the rest

period was chosen to be long enough for identification of differences in the poststimulus response between trials, while allowing a sufficient number of trials to be presented in the study.

Analysis. ***EEG.*** After filtering into the mu (8–13 Hz) frequency band, an EEG beamformer (51) was used to localize the mu response to MNS in the contralateral sensorimotor cortex. Virtual electrode time courses of single-trial mu activity were extracted, and the mean stimulus response (0–9.5 s), PERS (10.5–20 s), and control window (25–29.5 s) mu power values were calculated. For each subject, trials were sorted into lower (0–25%), median (37.5–62.5%), and upper (75–100%) quartiles based on PERS, stimulus response, or control window mu power.

fMRI. Regions of interest were defined from significant general linear model-identified responses to MNS in contralateral and ipsilateral sensorimotor cortex for each subject, and BOLD and CBF single-trial HRs extracted. For each subject, single-trial HRs were converted to percentage signal change relative to the amplitude of the final 6 s of the mean HR over all trials. HRs were sorted into quartiles according to the PERS, stimulus response, or control window mu power and averaged over subjects. For each quartile, the change in $CMRO_2$ during the poststimulus period was calculated using the Davis model (28) based on the individual subject's BOLD and CBF percentage signal changes from the mean baseline. See *SI Materials and Methods* for more detail on data acquisition and analysis.

ACKNOWLEDGMENTS. Funding for this work was provided by Medical Research Council Grant G0901321 and Engineering and Physical Science Research Council (EPSRC) Grants EP/F023057/1 and EP/J006823/1. K.J.M. was funded by a University of Nottingham Mansfield Fellowship and Anne McLaren Fellowship. S.D.M. was funded by EPSRC Fellowship EP/I022325/1 and a University of Birmingham Fellowship.

1. Ogawa S, et al. (1993) Functional brain mapping by blood oxygenation level-dependent contrast magnetic resonance imaging. A comparison of signal characteristics with a biophysical model. *Biophys J* 64(3):803–812.
2. Logothetis NK (2008) What we can do and what we cannot do with fMRI. *Nature* 453(7197):869–878.
3. Sadaghiani S, Hesselmann G, Friston KJ, Kleinschmidt A (2010) The relation of ongoing brain activity, evoked neural responses, and cognition. *Front Syst Neurosci* 4:20.
4. Aguirre GK, Zarahn E, D'esposito M (1998) The variability of human, BOLD hemodynamic responses. *Neuroimage* 8(4):360–369.
5. Duann JR, et al. (2002) Single-trial variability in event-related BOLD signals. *Neuroimage* 15(4):823–835.
6. Buxton RB, Uludağ K, Dubowitz DJ, Liu TT (2004) Modeling the hemodynamic response to brain activation. *Neuroimage* 23(Suppl 1):S220–S233.
7. Goense JB, Logothetis NK (2008) Neurophysiology of the BOLD fMRI signal in awake monkeys. *Curr Biol* 18(9):631–640.
8. Jin T, Kim SG (2008) Cortical layer-dependent dynamic blood oxygenation, cerebral blood flow and cerebral blood volume responses during visual stimulation. *Neuroimage* 43(1):1–9.
9. Yacoub E, Ugurbil K, Harel N (2006) The spatial dependence of the poststimulus undershoot as revealed by high-resolution BOLD- and CBV-weighted fMRI. *J Cereb Blood Flow Metab* 26(5):634–644.
10. Chen JJ, Pike GB (2009) Origins of the BOLD post-stimulus undershoot. *Neuroimage* 46(3):559–568.
11. Donahue MJ, et al. (2009) Cerebral blood flow, blood volume, and oxygen metabolism dynamics in human visual and motor cortex as measured by whole-brain multimodal magnetic resonance imaging. *J Cereb Blood Flow Metab* 29(11):1856–1866.
12. Frahm J, et al. (2008) The post-stimulation undershoot in BOLD fMRI of human brain is not caused by elevated cerebral blood volume. *Neuroimage* 40(2):473–481.
13. Sadaghiani S, Uğurbil K, Uludağ K (2009) Neural activity-induced modulation of BOLD poststimulus undershoot independent of the positive signal. *Magn Reson Imaging* 27(8):1030–1038.
14. Zong X, Huang J (2011) Linear coupling of undershoot with BOLD response in ER-fMRI and nonlinear BOLD response in rapid-presentation ER-fMRI. *Neuroimage* 57(2):391–402.
15. Buxton RB, Wong EC, Frank LR (1998) Dynamics of blood flow and oxygenation changes during brain activation: the balloon model. *Magn Reson Med* 39(6):855–864.
16. Lu H, Golay X, Pekar JJ, Van Zijl PCM (2004) Sustained poststimulus elevation in cerebral oxygen utilization after vascular recovery. *J Cereb Blood Flow Metab* 24(7):764–770.
17. Brockhaus J, Ballanyi K, Smith JC, Richter DW (1993) Microenvironment of respiratory neurons in the in vitro brainstem-spinal cord of neonatal rats. *J Physiol* 462:421–445.
18. Uludağ K, et al. (2004) Coupling of cerebral blood flow and oxygen consumption during physiological activation and deactivation measured with fMRI. *Neuroimage* 23(1):148–155.
19. Shmuel A, Augath M, Oeltermann A, Logothetis NK (2006) Negative functional MRI response correlates with decreases in neuronal activity in monkey visual area V1. *Nat Neurosci* 9(4):569–577.
20. Kastrup A, et al. (2008) Behavioral correlates of negative BOLD signal changes in the primary somatosensory cortex. *Neuroimage* 41(4):1364–1371.
21. Shmuel A, et al. (2002) Sustained negative BOLD, blood flow and oxygen consumption response and its coupling to the positive response in the human brain. *Neuron* 36(6):1195–1210.
22. Jurkiewicz MT, Gaetz WC, Bostan AC, Cheyne D (2006) Post-movement beta rebound is generated in motor cortex: Evidence from neuromagnetic recordings. *Neuroimage* 32(3):1281–1289.
23. Salmelin R, Hari R (1994) Spatiotemporal characteristics of sensorimotor neuromagnetic rhythms related to thumb movement. *Neuroscience* 60(2):537–550.
24. Stevenson CM, Brookes MJ, Morris PG (2011) β-Band correlates of the fMRI BOLD response. *Hum Brain Mapp* 32(2):182–197.
25. Cassim F, et al. (2001) Does post-movement beta synchronization reflect an idling motor cortex? *Neuroreport* 12(17):3859–3863.
26. Klimesch W, Sauseng P, Hanslmayr S (2007) EEG alpha oscillations: The inhibition-timing hypothesis. *Brain Res Brain Res Rev* 53(1):63–88.
27. Salenius S, Schnitzler A, Salmelin R, Jousmäki V, Hari R (1997) Modulation of human cortical rolandic rhythms during natural sensorimotor tasks. *Neuroimage* 5(3):221–228.
28. Davis TL, Kwong KK, Weisskoff RM, Rosen BR (1998) Calibrated functional MRI: Mapping the dynamics of oxidative metabolism. *Proc Natl Acad Sci USA* 95(4):1834–1839.
29. Chiarelli PA, Bulte DP, Piechnik SK, Jezzard P (2007) Sources of systematic bias in hypercapnia-calibrated functional MRI estimation of oxygen metabolism. *Neuroimage* 34(1):35–43.
30. Mandeville JB, et al. (1999) Evidence of a cerebrovascular postarteriole windkessel with delayed compliance. *J Cereb Blood Flow Metab* 19(6):679–689.
31. Hyder F, Rothman DL (2011) Evidence for the importance of measuring total brain activity in neuroimaging. *Proc Natl Acad Sci USA* 108(14):5475–5476.
32. Shulman RG, Rothman DL, Hyder F (2007) A BOLD search for baseline. *Neuroimage* 36(2):277–281.
33. Brookes MJ, et al. (2011) Investigating the electrophysiological basis of resting state networks using magnetoencephalography. *Proc Natl Acad Sci USA* 108(40):16783–16788.
34. De Luca M, Beckmann CF, De Stefano N, Matthews PM, Smith SM (2006) fMRI resting state networks define distinct modes of long-distance interactions in the human brain. *Neuroimage* 29(4):1359–1367.
35. von Stein A, Sarnthein J (2000) Different frequencies for different scales of cortical integration: From local gamma to long range alpha/theta synchronization. *Int J Psychophysiol* 38(3):301–313.
36. Bressler SL, Menon V (2010) Large-scale brain networks in cognition: Emerging methods and principles. *Trends Cogn Sci* 14(6):277–290.
37. Romei V, et al. (2008) Spontaneous fluctuations in posterior alpha-band EEG activity reflect variability in excitability of human visual areas. *Cereb Cortex* 18(9):2010–2018.
38. Leocani L, Toro C, Zhuang P, Gerloff C, Hallett M (2001) Event-related desynchronization in reaction time paradigms: A comparison with event-related potentials and corticospinal excitability. *Clin Neurophysiol* 112(5):923–930.
39. Chen R, Hallett M (1999) The time course of changes in motor cortex excitability associated with voluntary movement. *Can J Neurol Sci* 26(3):163–169.
40. Hummel F, Andres F, Altenmüller E, Dichgans J, Gerloff C (2002) Inhibitory control of acquired motor programmes in the human brain. *Brain* 125(Pt 2):404–420.
41. Yuan H, Perdoni C, Yang L, He B (2011) Differential electrophysiological coupling for positive and negative BOLD responses during unilateral hand movements. *J Neurosci* 31(26):9585–9593.
42. Babiloni C, et al. (2002) Human cortical electroencephalography (EEG) rhythms during the observation of simple aimless movements: A high-resolution EEG study. *Neuroimage* 17(2):559–572.
43. Duff E, et al. (2007) Complex spatio-temporal dynamics of fMRI BOLD: A study of motor learning. *Neuroimage* 34(1):156–168.
44. Huang RS, Jung TP, Makeig S (2007) Event-related brain dynamics in continuous sustained-attention tasks. *Lect Notes Artif Int* 4565:65–74.
45. Zumer JM, Brookes MJ, Stevenson CM, Francis ST, Morris PG (2010) Relating BOLD fMRI and neural oscillations through convolution and optimal linear weighting. *Neuroimage* 49(2):1479–1489.
46. Magri C, Schridde U, Murayama Y, Panzeri S, Logothetis NK (2012) The amplitude and timing of the BOLD signal reflects the relationship between local field potential power at different frequencies. *J Neurosci* 32(4):1395–1407.
47. Başar E, Schürmann M, Başar-Eroglu C, Karakaş S (1997) Alpha oscillations in brain functioning: An integrative theory. *Int J Psychophysiol* 26(1–3):5–29.
48. Walter W (1950) Normal rhythms: Their development, disruption and significance. *Electroencephalography*, eds Hill D, Parr G (McDonald, London).
49. Klingner CM, Hasler C, Brodoehl S, Witte OW (2010) Dependence of the negative BOLD response on somatosensory stimulus intensity. *Neuroimage* 53(1):189–195.
50. Wesolowski R, Gowland PA, Francis ST (2009) Double acquisition background suppressed (DABS) FAIR at 3T and 7T: Advantages for simultaneous BOLD and CBF Acquisition. *Proc ISMRM*. Available at http://cds.ismrm.org/protected/09MProceedings/files/01526.pdf.
51. Brookes MJ, Mullinger KJ, Stevenson CM, Morris PG, Bowtell R (2008) Simultaneous EEG source localisation and artifact rejection during concurrent fMRI by means of spatial filtering. *Neuroimage* 40(3):1090–1104.